

## Article

# Environmental Persistence of the Antidepressant Fluoxetine and Its Pharmaceutical Alternative: Kinetics of Oxidation and Mathematical Simulations

Larissa P. Souza <sup>1,\*</sup> , João G. M. Carneiro <sup>1</sup> , Arlen M. Lastre-Acosta <sup>1,2</sup> , Bruno Ramos <sup>1,3</sup>   
and Antonio C. S. C. Teixeira <sup>1,\*</sup> 

<sup>1</sup> Research Group in Advanced Oxidation Processes (AdOx), Department of Chemical Engineering, Escola Politécnica, University of Sao Paulo, Sao Paulo 05508-010, SP, Brazil

<sup>2</sup> Agência Ambiental do Vale do Paraíba, Rua Euclides Miragaia, 433, Sala 201–Edifício Cristal Center–Centro, São José dos Campos 12210-110, SP, Brazil

<sup>3</sup> Department of Metallurgical and Materials Engineering, Escola Politécnica, University of São Paulo, Sao Paulo 05508-010, SP, Brazil

\* Correspondence: larissapdesouza@usp.br (L.P.S.); acscteix@usp.br (A.C.S.C.T.)

**Abstract:** To investigate the impact of antidepressants (ANT) in water, estimates of the direct and indirect photolysis of standard fluoxetine hydrochloride (FLX) and a pharmaceutical alternative, fluoxetine sulfate (FLXSO<sub>4</sub>), were evaluated. The second-order kinetic constants of the ANT and reactive photoinduced species (RPS) (singlet oxygen, <sup>1</sup>O<sub>2</sub>; hydroxyl radicals, HO•; and triplet excited states of chromophoric dissolved organic matter, <sup>3</sup>CDOM\*) were obtained by competition kinetics under simulated solar radiation. These parameters were used in combination with water characteristics to assess the environmental persistence of the ANT based on mathematical kinetic simulations. The results indicated that the reactions with HO• ( $k_{\text{FLX},\text{HO}\cdot} = (2.54 \pm 0.06) \times 10^9 \text{ L mol}^{-1} \text{ s}^{-1}$ ;  $k_{\text{FLXSO}_4,\text{HO}\cdot} = (3.07 \pm 0.03) \times 10^9 \text{ L mol}^{-1} \text{ s}^{-1}$ ) and <sup>3</sup>CDOM\* ( $k_{\text{FLX},^3\text{CDOM}^*} = (2.67 \pm 0.05) \times 10^9 \text{ L mol}^{-1} \text{ s}^{-1}$ ;  $k_{\text{FLXSO}_4,^3\text{CDOM}^*} = (1.48 \pm 0.03) \times 10^9 \text{ L mol}^{-1} \text{ s}^{-1}$ ) play a more important role in the degradation of ANT compared to the reactions with <sup>1</sup>O<sub>2</sub> ( $k_{\text{FLX},^1\text{O}_2} = (1.37 \pm 0.07) \times 10^7 \text{ L mol}^{-1} \text{ s}^{-1}$ ;  $k_{\text{FLXSO}_4,^1\text{O}_2} = (1.63 \pm 0.33) \times 10^7 \text{ L mol}^{-1} \text{ s}^{-1}$ ). The main removal pathways were biodegradation and direct photolysis with persistence in the following order FLX > FLXSO<sub>4</sub>. Therefore, the presence of sulfate anions can contribute to the degradation of fluoxetine in sunlit environmental waters.

**Keywords:** antidepressants; photolysis; photoinduced reactive species (RPS); competition kinetics; photochemical environmental persistence; real matrix; Guarapiranga reservoir; environmental modeling; APEX model



**Citation:** Souza, L.P.; Carneiro, J.G.M.; Lastre-Acosta, A.M.; Ramos, B.; Teixeira, A.C.S.C. Environmental Persistence of the Antidepressant Fluoxetine and Its Pharmaceutical Alternative: Kinetics of Oxidation and Mathematical Simulations. *Water* **2022**, *14*, 3536. <https://doi.org/10.3390/w14213536>

Academic Editor: Cátia A. L. Graça

Received: 21 September 2022

Accepted: 31 October 2022

Published: 3 November 2022

**Publisher's Note:** MDPI stays neutral with regard to jurisdictional claims in published maps and institutional affiliations.



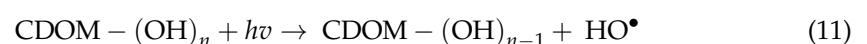
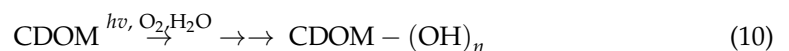
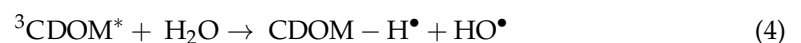
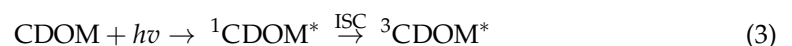
**Copyright:** © 2022 by the authors. Licensee MDPI, Basel, Switzerland. This article is an open access article distributed under the terms and conditions of the Creative Commons Attribution (CC BY) license (<https://creativecommons.org/licenses/by/4.0/>).

## 1. Introduction

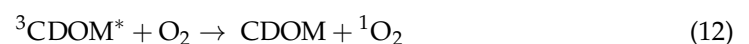
The growing worldwide contamination of water bodies by antidepressants in recent years has placed this class of compounds in a position of emerging concern. The COVID-19 pandemic caused psychological disorders such as anxiety, depression, insomnia, and post-traumatic stress disorder that increased their consumption in the last few years [1,2]. Among the first therapeutic options to address these disorders are selective serotonin reuptake inhibitors (SSRIs), drugs that act by modulating the distribution of serotonin in the central nervous system. Fluoxetine hydrochloride (FLX) is one of the most commonly consumed SSRIs worldwide [1], ranking 20th on the list of the 200 most prescribed drugs in the United States (US) [3]. As a result of high consumption, the occurrence of this drug has already been observed in different environments and concentrations, such as 7.6–20 ng L<sup>-1</sup> (municipal wastewater treatment plant-WWTP influent, Canada [4]); 600–100 ng L<sup>-1</sup> (WWTP influent/effluent, Costa Rica [5]); 7.5–750 ng L<sup>-1</sup> (WWTP influent, Belgium [6]); 50–58 ng L<sup>-1</sup> (WWTP influent, London/UK [7]); 4.7–9.4 ng L<sup>-1</sup> (Dal

River/Sweden [8]); 2.1–19.5 ng L<sup>-1</sup> (Lis River/Portugal [9]); and 0.58 ng L<sup>-1</sup> (sea, Santos Bay/Brazil [10]). FLX can be introduced into the environment as a result of various anthropogenic sources, the main one being the irregular domestic disposal of expired drugs, incomplete absorption followed by physiological elimination, and the direct disposal of partially treated pharmaceutical effluents [11]. In the human body, the excretion of FLX and its main metabolite (norfluoxetine) occurs mainly through urine [12]. Once discharged into domestic or industrial wastewater, the removal of these drugs poses a significant technological challenge since the processes used in conventional wastewater treatment plants (WWTP) have shown low removal efficiency [13–15]. Once released into the environment, FLX can cause adverse effects in fish, crayfish, marine rotifers, hydra, clams, and mussels [1]. In view of the potentially harmful effects caused by FLX, countries such as Switzerland already include antidepressants in the list of priority compounds to monitor before release into urban wastewater [16].

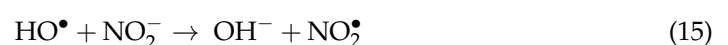
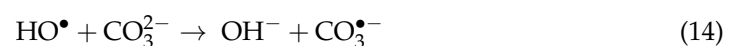
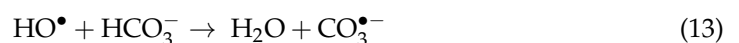
In this sense, the study of the kinetics of oxidation of these compounds by direct and indirect photolysis is especially important to understand their behavior when exposed to sunlight, the main driver of their degradation in natural waters [17,18]. The use of these parameters in mathematical simulations has been widely discussed in the literature [19,20] and can provide valuable information on the environmental photochemical persistence of these compounds. When there is an overlap between the sunlight spectrum, the absorption spectrum of the pollutant, and its photolysis quantum yield, an organic contaminant will photolyze directly under environmental conditions. On the other hand, photoinduced reactive species (RPS), such as singlet oxygen (<sup>1</sup>O<sub>2</sub>), hydroxyl radicals (HO•), and triplet excited states of chromophoric dissolved organic matter (<sup>3</sup>CDOM\*) that are formed in surface water as a result of light absorption by its constituents (i.e., nitrate and nitrite ions, dissolved organic matter) are what causes indirect photolysis [21]. The chemistry behind the formation of HO• can be summarized by the following reactions [20–23]:

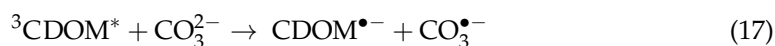


Furthermore, the generation of <sup>1</sup>O<sub>2</sub> by energy transfer between <sup>3</sup>CDOM\* and dissolved oxygen is possible [24]:



Finally, the interaction of RPS with water constituents allows the formation of secondary species [20]:





Despite the importance of oxidation kinetics to understand the environmental fate of the antidepressants, few studies have been carried out in the literature in this regard [17,25–27], and only Lam et al. [28] focused on FLX, although with limitations in the number of RPSs studied. The simulation approach through photochemical models, although not as common, can predict the fate of these compounds satisfactorily. The APEX (Aqueous Photochemistry of Environmentally Occurring Xenobiotics) software is used for this purpose in several literature publications [19,20], which was used to calculate the persistence of paroxetine [17] and sertraline [26], the only antidepressants studied by this approach. Despite the valuable contribution of APEX to the studies of environmental photochemical persistence, a major concern has been the representativeness of the models in relation to key real conditions that consider weather-related phenomena, such as seasonal effects, the contribution of insolation, and relevant water constituents, among others [20,29]. In this sense, a recent work was published on the antidepressant venlafaxine [27], demonstrating the impact of using more realistic conditions on the modeling results.

To fill the gaps in the kinetics of FLX photo-oxidation in natural waters and the prediction of its environmental photochemical fate based on real weather and environmental conditions, our research objectives were to: (i) investigate the direct photolysis of FLX and its reactions with reactive photoinduced species (RPS), that is,  $\text{HO}^\bullet$ ,  ${}^3\text{CDOM}^*$  and  ${}^1\text{O}_2$ , under simulated sunlight; (ii) expand the APEX code to predict FLX half-life times in an important water reservoir in the São Paulo Metropolitan Region (Guarapiranga reservoir), based on experimental results and local measurements of insolation, seasonal weather conditions and water quality parameters, including the contributions of adsorption and biodegradation to the persistence of antidepressants; (iii) assess the environmental persistence of a pharmaceutical alternative fluoxetine sulfate ( $\text{FLXSO}_4$ ), proposed to increase the absorption of the drug in the human organism, and compare with the results obtained for fluoxetine hydrochloride (FLX); (iv) evaluate the photodegradation of antidepressants (FLX and  $\text{FLXSO}_4$ ) by the action of sunlight on a real natural water sample (Guarapiranga reservoir, Brazil).

## 2. Materials and Methods

### 2.1. Experimental Procedures

#### 2.1.1. Chemicals

All of the reactants were of analytical grade. FLX (fluoxetine,  $\text{C}_{17}\text{H}_{18}\text{F}_3\text{NO}\cdot\text{HCl}$ ) was supplied by Campos Manipulação in the form of hydrochloride salt.  $\text{FLXSO}_4$  (modified fluoxetine,  $((\text{C}_{17}\text{H}_{18}\text{F}_3\text{NO})_2\text{SO}_4)$ ) was supplied by the Institute of Physics of the Federal University of Mato Grosso do Sul (IF/UFMS) in the form of sulfate salt. Methylene blue from Synth and furfuryl alcohol (FFA) from Sigma-Aldrich were used to determine the kinetics of antidepressant oxidation by  ${}^1\text{O}_2$ . Hydrogen peroxide ( $\text{H}_2\text{O}_2$ ) and para-chlorobenzoic acid (pCBA), obtained from Synth and Sigma-Aldrich, respectively, were used to assess the kinetics of antidepressant oxidation by  $\text{HO}^\bullet$  radicals. The kinetics of reactions between antidepressants and  ${}^3\text{CDOM}^*$  were determined using 4-carboxybenzophenone (CBBP) and 2,4,6-trimethylphenol (TMP) from Sigma-Aldrich, with CBBP used as a proxy for CDOM [29]. All solutions were prepared in water from a Milli-Q® Direct-Q system (18.2 M cm) (Merck Millipore).

#### 2.1.2. Natural Water Sampling

Experiments were also performed with natural water from the Guarapiranga reservoir (SP, Brazil) to evaluate the impact of a variety of species, present in a real matrix (organic matter and inorganic species), on the photodegradation of antidepressants. The samples were collected in May 2022 by the (São Paulo) State Environmental Company (CETESB).

The point chosen for sampling was GUAR00100 (23°45'15" S, 46°43'37" W), which is a highly urbanized area according to [30]. The collected samples were stored in amber glass bottles and kept under refrigeration until analysis. The physicochemical parameters of this sample are summarized in Table S1 and were provided by [30].

### 2.1.3. Photolysis under Simulated Sunlight

The photolysis experiments were carried out with the help of a solar simulator (PEC-L01, Peccell Technologies, Inc., Yokohama, Japan) equipped with an AM 1.5 global filter. Reactions were conducted in 2-mL Pyrex vials with an irradiated path length of 10 mm and no head space. When filling the vials with solution, care was taken to remove bubbles. The contents of the vials were thoroughly mixed immediately before being placed in a water bath at 21 °C, 15 cm from the radiation source (Figure S1). The total irradiance at this distance was 43 W m<sup>-2</sup> (290–800 nm) measured by a spectroradiometer (model SPR-02, Luzchem Research, Inc., Ottawa, ON, Canada). The initial concentration of antidepressants was set at [FLX]<sub>0</sub> = 10 mg L<sup>-1</sup> (28.9 μmol L<sup>-1</sup>) and [FLXSO<sub>4</sub>]<sub>0</sub> = 10 mg L<sup>-1</sup> (13.9 μmol L<sup>-1</sup>), which is suitable for kinetic competition experiments, ensuring immediate quantification by high-performance liquid chromatography (HPLC) without the need for pre-concentration steps. The runs were performed at selected times (0.5, 1, 2, 3, 5, 15, 30, 60, and 120 min), with the solution inside the vial being analyzed at the end of each time. At natural pH (FLX: ~6.7; FLXSO<sub>4</sub>: ~6.3), all assays were repeated in duplicate. Finally, the quantum yield was quantified using the methodology described in [27].

### 2.1.4. Competition Kinetic Experiments under Simulated Sunlight

The photodegradation experiments were conducted using a radiation source that simulates solar radiation, with a 400 W mercury iodide lamp (Master HPI-T Plus, Philips—Amsterdam, The Netherlands). The reactions were carried out with the same experimental procedure described in Section 2.1.3 (Figure S1). However, the distance from the radiation source was 11 cm to ensure that the total irradiance at this distance was 43 W m<sup>-2</sup> (290–800 nm).

Then, the second-order kinetic rate constants between the antidepressants (ANT) and reactive photoinduced species (RPS), namely, singlet oxygen (<sup>1</sup>O<sub>2</sub>), hydroxyl radicals (HO•), and triplet excited states of chromophoric dissolved organic matter (<sup>3</sup>CDOM\*), were determined by competition kinetics [31]. The method is based on the competition between the target contaminant (FLX and FLXSO<sub>4</sub>) and the reference compound (FFA, pCBA, or TMP, respectively) for RPS (<sup>1</sup>O<sub>2</sub>, HO•, or <sup>3</sup>CDOM\*, respectively), whose reactivity towards the particular RPS is known. Thus, the second-order kinetic rate constant can be calculated as:

$$k_{ANT,RPS} = \frac{k_{ANT(obs)} - k_{ANT(direct\ phot)}}{k_{ref(obs)} - k_{ref(direct\ phot)}} \times k_{ref,RPS} \quad (19)$$

where the experimentally observed pseudo-first-order specific degradation rates of the antidepressant and the reference compound, respectively, are represented by  $k_{ANT(obs)}$  and  $k_{ref(obs)}$ , while  $k_{ANT(direct\ phot)}$  and  $k_{ref(direct\ phot)}$  are the measured first-order photolysis rate constants of the antidepressant and the reference compound, respectively. The second-order rate constant ( $k_{ref,RPS}$ ) between each reference compound and RPS is known from the literature as the following values:  $k_{FFA,^1O_2} = 1.2 \times 10^8 \text{ L mol}^{-1} \text{ s}^{-1}$  [32],  $k_{pCBA,HO\bullet} = 5 \times 10^9 \text{ L mol}^{-1} \text{ s}^{-1}$  [33], and  $k_{TMP,^3CDOM^*} = 3 \times 10^9 \text{ L mol}^{-1} \text{ s}^{-1}$  [34]. H<sub>2</sub>O<sub>2</sub> (50 mmol L<sup>-1</sup>), methylene blue (31.3 μmol L<sup>-1</sup>), and 4-carboxybenzophenone (CBBP) (44.2 μmol L<sup>-1</sup>), in that order, were the sources of HO•, <sup>1</sup>O<sub>2</sub>, and <sup>3</sup>CDOM\*. The amounts of H<sub>2</sub>O<sub>2</sub>, methylene blue, and CBBP were based on previous investigations to ensure the formation of excess RPS for competition between the antidepressants and reference substances [35]. *Para*-chlorobenzoic acid (pCBA) (FLX system: 28.9 μmol L<sup>-1</sup>; FLXSO<sub>4</sub> system: 24.7 μmol L<sup>-1</sup>), furfuryl alcohol (FFA) (FLX system: 28.9 μmol L<sup>-1</sup>; FLXSO<sub>4</sub> system: 24.7 μmol L<sup>-1</sup>), and 2,4,6 trimethylphenol (TMP) (FLX system: 28.9 μmol L<sup>-1</sup>; FLXSO<sub>4</sub> system: 24.7 μmol L<sup>-1</sup>) were used as the reference compounds for HO•, <sup>1</sup>O<sub>2</sub>,

and  $^3\text{CDOM}^*$ , respectively. Methanol ( $0.1 \text{ mol L}^{-1}$ ) was added as needed to quench hydroxyl radicals. All competition kinetic experiments were performed in duplicates at pH 4.4 (FLX + pCBA +  $\text{H}_2\text{O}_2$ ), 5.1 (FLX + FFA + methylene blue + MeOH), 6.1 (FLX + TMP + CBBP), 4.1 (FLXSO<sub>4</sub> + pCBA +  $\text{H}_2\text{O}_2$ ), 4.8 (FLXSO<sub>4</sub> + FFA + methylene blue + MeOH), and 5.9 (FLXSO<sub>4</sub> + TMP + CBBP), which correspond to the natural initial pH of each system and were not controlled over time.

#### 2.1.5. Analytical Methods

An ultrafast liquid chromatography (UFLC) system (UFLC LC-20AD, Shimadzu—Kyoto, Japan) was used to measure the concentrations of antidepressants (FLX and FLXSO<sub>4</sub>) and reference compounds (FFA, pCBA, and TMP) using a C18 column ( $4.6 \text{ mm} \times 250 \text{ mm}$ ,  $5 \mu\text{m}$ ), 70% acetonitrile (ACN):30%  $\text{H}_2\text{O}$  (1% trifluoroacetic acid, TFA), at a flow rate of  $1.0 \text{ mL min}^{-1}$ . The column temperature was kept at  $40 \text{ }^\circ\text{C}$ , and the injection volume was  $50 \mu\text{L}$ . The detection wavelengths for FLX, FLXSO<sub>4</sub>, pCBA, FFA, and TMP were 230, 227, 234, 219, and 222 nm, respectively. Retention times (RT), limits of detection (LOD), and limits of quantification (LOQ) were obtained using this analytical technique and are displayed in Table S2.

### 2.2. Modeling and Simulation

#### 2.2.1. Modeling Photochemical Persistence

Mathematical simulations of the photodegradation of the antidepressants in natural waters were performed based on the APEX (Aqueous Photochemistry of Environmentally Occurring Xenobiotics) code [20], with modifications to account for the impacts of geographic location and seasonality and also to incorporate other absorbing species that might hinder the local generation of RPSs as reported in [27]. Additionally, the partitioning of the contaminant between the suspended solids and the liquid phase (adsorption calculations) and biodegradation were incorporated in the present work (see details in Supplementary Information). Local estimates of clear sky irradiance were achieved by integrating the APEX code with the SMARTS (Simple Model of Atmospheric Radiative Transfer of Sunshine) model [36]. Variations in meteorological conditions were considered by combining the SMARTS model with typical meteorological year (TMY) data. The TMY data were retrieved from the Photovoltaic Geographic Information System (PVGIS) based on satellite images [37]. Additional terms were included in our previous work [27] to account for light attenuation by chlorophyll-*a*, turbidity caused by the presence of suspended solids,  $\epsilon_T$  [ $\text{m}^{-1}$ ], and the effect of dissolved oxygen levels, OD, [ $\text{mol L}^{-1}$ ] in the evaluation of the quantum yield of singlet oxygen ( $^1\text{O}_2$ ) generation by CDOM to consider eutrophication levels. In the first case, turbidity measurements (NTU) were correlated with photosynthetically active radiation (PAR, 400–700 nm) for lakes and dams [38]. On the other hand, terms related to the reduction in the pollutant concentration in the liquid phase, such as the distribution coefficient (solid/liquid) ( $K_d$ ) and the biodegradation rate ( $r_{X,\text{biodeg}}$ ) were considered for the first time in this work. To obtain  $K_d$ , the values of the fraction of organic carbon in solids ( $f_{oc}$ ) and the distribution coefficient for organic carbon ( $K_{od}$ ) were taken from [39] and the OPEn structure–activity/property Relationship App (OPERA), respectively. From the machine learning methods, with the PaDEL descriptors used by OPERA in its calculations, it is possible to estimate the biodegradation half-life, similarly to the  $K_{oc}$  value obtained for the modeling of adsorption. A mathematical explanation of the equations that were implemented in this modification can be seen in Supplementary Information.

#### 2.2.2. Simulation Conditions

The simulations were run using information gathered by the (São Paulo) State Environmental Company [30] at the point GUAR00100 ( $23^\circ 45' 15'' \text{ S}$ ,  $46^\circ 43' 37'' \text{ W}$ ) of the main body of the Guarapiranga Reservoir (gray point marker in Figure 1). Close to urban surroundings, the reservoir is affected by episodes of the inadequate disposal of waste into the environment or the diffuse discharge of untreated sewage into the drainage system [40].

The input data used in the simulations were collected in June and September 2021, as summarized in Table 1. The measured kinetic constants as described in the experimental section, in addition to a second order rate constant previously described for the reaction with carbonate radical anions ( $\text{CO}_3^{\bullet-}$ ),  $k_{\text{VNX},\text{CO}_3^{\bullet-}} = 4.86 \times 10^6 \text{ L mol}^{-1} \text{ s}^{-1}$  [41], were used in the simulations, considering an environmental concentration of  $[\text{FLX}]_0 = 6.96 \times 10^{-10} \text{ mol L}^{-1}$ , which is the average of the FLX concentrations found in the surface water [1,2].

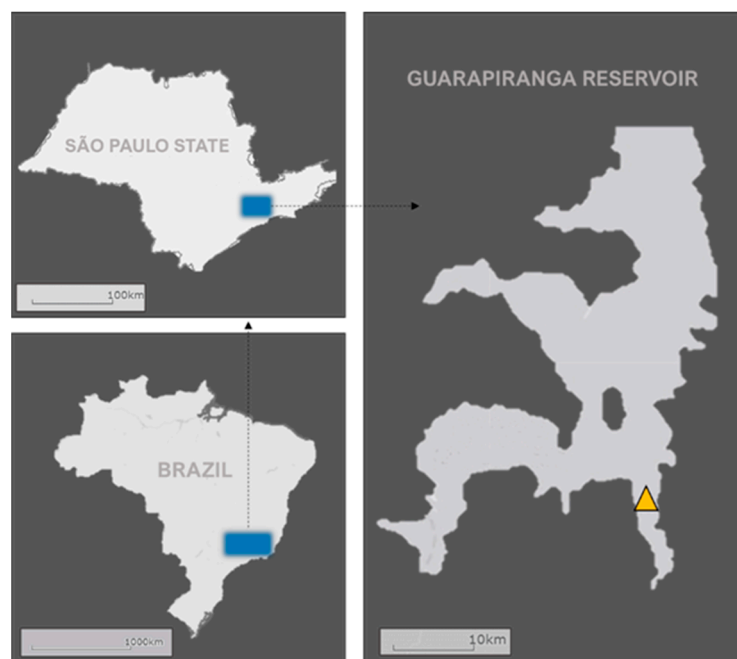


**Figure 1.** Location of the Guarapiranga reservoir. (▲) Sampling station from which the data used in the analysis were gathered.

**Table 1.** Variables used in the mathematical simulation of the photochemical persistence of antidepressants (FLX and  $\text{FLXSO}_4$ ) based on data collected from the Guarapiranga Reservoir in June and September 2021.

Parameter	June	September
Mean depth (m) <sup>1</sup>	5.7	5.7
Turbidity (NTU) <sup>2</sup>	5.2	11
pH <sup>2</sup>	6.5	6.8
Total suspended solids (TSS)	100	100
Water temperature (°C) <sup>2</sup>	18.5	23.4
Hardness (mg $\text{CaCO}_3$ ) <sup>2</sup>	43.1	41.2
Nitrates (mg $\text{L}^{-1}$ ) <sup>2</sup>	0.32	0.72
Nitrites (mg $\text{L}^{-1}$ ) <sup>2</sup>	0.12	0.11
TOC (mg $\text{L}^{-1}$ ) <sup>2</sup>	5.28	6.51
Total chlorine (mg $\text{L}^{-1}$ ) <sup>2</sup>	16	19.7
Chlorophyll- <i>a</i> (µg $\text{L}^{-1}$ ) <sup>2</sup>	61.4	74.84
Dissolved oxygen (mg $\text{L}^{-1}$ ) <sup>2</sup>	6.47	6.7
Fraction of organic carbon in solids ( $f_{\text{OC}}$ ) <sup>3</sup>	0.152	0.152

<sup>1</sup> The average historical water depth of the Guarapiranga Reservoir was considered as 5.7 m [40]; <sup>2</sup> Data gathered from the InfoAguas system (collection point GUAR00100) for the dates 29 June 2021 and 14 September 2021);

<sup>3</sup> Data gathered from [39].

### 3. Results and Discussions

#### 3.1. Photodegradation of Antidepressants under Simulated Sunlight

##### 3.1.1. Direct Photolysis

Control experiments confirmed that there was no significant reduction in the concentration of the antidepressants due to hydrolysis in pure water and natural pH (FLX: ~6.7; FLXSO<sub>4</sub>: ~6.3) (Figures S3 and S4). Low photolysis rates with  $k_{\text{FLX}} = (2.09 \pm 0.04) \times 10^{-4} \text{ min}^{-1}$  ( $R^2 = 0.9775$ ) and  $k_{\text{FLXSO}_4} = (1.30 \pm 0.40) \times 10^{-3} \text{ min}^{-1}$  ( $R^2 = 0.9387$ ) were observed for the antidepressants over 120 min at natural pH (Figure 2a), which is associated with their low photon absorptivity above 290 nm (Figure 2b). However, it is worth noting that the modification of the counterion (FLXSO<sub>4</sub>) increases the experimental molar absorption coefficient in the region of 360–600 nm and consequently enhances the photolysis rate (Figure 2b). Lam et al. [28] obtained very similar results for the simulated direct sunlight photolysis of FLX ( $k_{\text{obs}} = 2.10 \times 10^{-4} \text{ min}^{-1}$ ) with the occurrence of the defluorination of the trifluoromethyl group in the FLX and formation of O-dealkylation products.

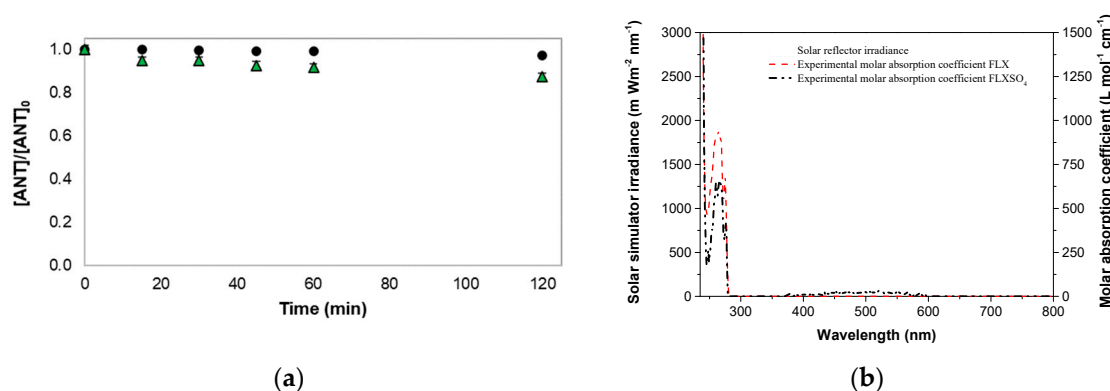


**Figure 2.** Direct photolysis of the antidepressants. (a) Decay of (●) FLX (▲) FLXSO<sub>4</sub> under simulated solar radiation; (b) Spectral irradiance of the solar simulator (left vertical axis) and spectral decadic molar absorption coefficient of ANT (FLX and FLXSO<sub>4</sub>) measured in this work (right vertical axis). Conditions:  $[\text{ANT}]_0 = (10.33 \pm 0.53) \text{ mg L}^{-1}$ ; natural pH (FLX: ~6.7; FLXSO<sub>4</sub>: ~6.3); pure water.

Based on these data, direct photolysis quantum yields were determined for FLX ( $\Phi = 1.04 \times 10^{-5} \text{ mol Einstein}^{-1}$ ) and FLXSO<sub>4</sub> ( $\Phi = 7.60 \times 10^{-4} \text{ mol Einstein}^{-1}$ ) following the approach used in previous works [42]. Similar results were obtained by [28] for the quantum yield of FLX direct photolysis ( $\Phi = 4.2 \times 10^{-5} \text{ mol Einstein}^{-1}$ ).

##### 3.1.2. Indirect Photolysis

Table 2 presents the results of indirect photolysis under simulated solar radiation for the antidepressants. Reactions with HO• and <sup>3</sup>CDOM\* play a more important role in the degradation of the antidepressants compared to <sup>1</sup>O<sub>2</sub>, as  $k_{\text{ANT},^1\text{O}_2}$  is much lower than the values of the  $k_{\text{ANT},\text{HO}\cdot}$  and  $k_{\text{ANT},^3\text{CDOM}^*}$  obtained. The value of  $k_{\text{FLX},\text{HO}\cdot}$  is of the same order of magnitude as the values presented in the work of Lam et al. [28] by two different kinetic competition methods, namely,  $k_{\text{FLX},\text{HO}\cdot} = (8.4 \pm 0.5) \times 10^9 \text{ L mol}^{-1} \text{ s}^{-1}$  and  $k_{\text{FLX},\text{HO}\cdot} = (9.6 \pm 0.8) \times 10^9 \text{ L mol}^{-1} \text{ s}^{-1}$ , which confirms the validity of the results obtained. The values of  $k_{\text{FLX},^1\text{O}_2}$  and  $k_{\text{FLX},^3\text{CBBP}^*}$  were not found in the literature for comparison purposes with our study. However, a similar behavior, concerning the predominance of HO• on indirect photodegradation, was observed by Gornik et al. [26] for the antidepressant paroxetine and by Lam et al. [28] with the production of hydroxylated and O-dealkylated byproducts. Similarly to what was observed in direct photolysis, the addition of a different counterion (FLXSO<sub>4</sub>) promoted increases of 20.9% and 2.1% in the reaction rate constants with HO• and <sup>1</sup>O<sub>2</sub>, respectively, which can be explained by the synergistic action of a higher value of direct photolysis associated with a lower kinetic competition observed between FLXSO<sub>4</sub> and the reference compounds. On the other hand, the reaction rate constants with <sup>3</sup>CDOM\*

were reduced by 38.9% with the replacement of the counterion, leading to the hypothesis that the modification in the counterion provides greater kinetic competition with organic matter. Therefore, for a better understanding of the role of FLXSO<sub>4</sub> as an environmentally safer form of FLX, the evaluation of its behavior in a real water matrix is necessary.

**Table 2.** Second-order kinetic rate constants of the reactions between antidepressants (ANT) and reactive photoinduced species (<sup>1</sup>O<sub>2</sub>, HO•, <sup>3</sup>CBBP\*) in pure water at natural pH.

ANT	$k_{\text{ANT},\text{HO}\cdot}$ (10 <sup>9</sup> L mol <sup>-1</sup> s <sup>-1</sup> )	$k_{\text{ANT},^1\text{O}_2}$ (10 <sup>7</sup> L mol <sup>-1</sup> s <sup>-1</sup> )	$k_{\text{ANT},^3\text{CBBP}^*}$ (10 <sup>9</sup> L mol <sup>-1</sup> s <sup>-1</sup> ) <sup>1</sup>
FLX	2.54 ± 0.06	1.37 ± 0.07	2.67 ± 0.05
FLXSO <sub>4</sub>	3.07 ± 0.03	1.63 ± 0.33	1.48 ± 0.03

<sup>1</sup>3CBBP\* corresponds to the triplet excited state of 4-carboxybenzophenone used as CDOM proxy [43].

### 3.2. Photodegradation of Antidepressants in the Water of the Guarapiranga Reservoir

Control experiments in the dark (natural pH and kept at 24 °C) confirmed the chemical stability of both antidepressants (FLX and FLXSO<sub>4</sub>) in the water of the Guarapiranga reservoir without an appreciable reduction in their initial concentrations due to hydrolysis. Thus, antidepressant decrease in the concentration observed upon irradiation occurred only by the interaction with UV-visible radiation and/or by the mechanisms of indirect photochemical processes promoted by RPS. Therefore, to investigate more representatively what occurs in the natural environment, the performance of distinct species (organic matter, inorganic species) that affect the photodegradation of contaminants in aqueous environments was evaluated through the photolysis of antidepressants in a natural water sample. Antidepressant solutions were prepared in water from the Guarapiranga reservoir ([ANT]<sub>0</sub> = (10.67 ± 0.49) mg L<sup>-1</sup> and natural pH = 7.2) and irradiated for 120 min under simulated solar radiation with an uncontrolled natural initial pH over time.

Figure 3 shows an increase in the degradation of antidepressants in natural water compared to that observed in pure water, suggesting the appearance of additional indirect photochemical processes and/or biodegradation. The removal of FLX in the real matrix was 12.7% ( $k_{\text{obs}} = (1.34 \pm 0.52) \times 10^{-3} \text{ min}^{-1}$ ;  $R^2 = 0.9114$ ) compared to 2.7% ( $k_{\text{obs}} = (2.09 \pm 0.40) \times 10^{-4} \text{ min}^{-1}$ ;  $R^2 = 0.9775$ ) in pure water. An even more expressive removal behavior was observed for FLXSO<sub>4</sub> with 20.7% ( $k_{\text{obs}} = (2.23 \pm 0.20) \times 10^{-3} \text{ min}^{-1}$ ;  $R^2 = 0.9387$ ) in the real matrix compared to 12.6% ( $k_{\text{obs}} = (1.30 \pm 0.45) \times 10^{-3} \text{ min}^{-1}$ ;  $R^2 = 0.9387$ ) in pure water.

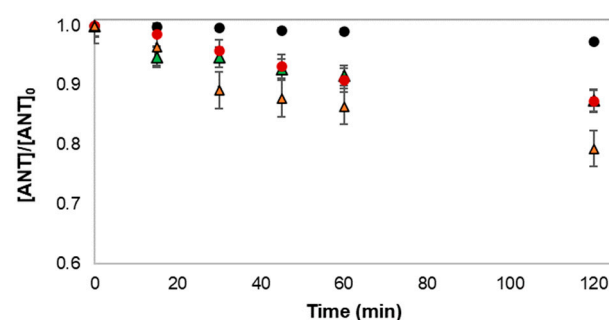


**Figure 3.** Photolysis under simulated solar radiation (43 W m<sup>-2</sup>, 290–800 nm) at 21 °C. Guarapiranga reservoir matrix (pH 7.2): (●) FLX (▲) FLXSO<sub>4</sub>; Pure water matrix (natural pH: FLX: ~6.7; FLXSO<sub>4</sub>: ~6.3): (●) FLX (▲) FLXSO<sub>4</sub>. [ANT]<sub>0</sub> = (10.67 ± 0.49) mg L<sup>-1</sup>. Experiments were performed in duplicate.

The presence of organic matter, inorganic species, and biological organisms (Table S1) may explain the significant difference between the percentage removal of ANT in natural and pure water matrices due to the hypothesis of the additional formation of different RPSs and biodegradation. The significant removal of FLXSO<sub>4</sub> can be explained by an association



of direct photolysis processes (more expressive in the case of FLXSO<sub>4</sub> than in FLX due to its higher quantum yield and molar absorptivity coefficients in the irradiated region), as well as the interaction of the sulfate ions with reactive species formed in the natural water matrix, for example, the formation of sulfate radicals (SO<sub>4</sub><sup>•−</sup>) through the interaction of SO<sub>4</sub><sup>2−</sup> with HO<sup>•</sup> radicals ( $k_{\text{obs}} = 6.9 \times 10^5 \text{ L mol}^{-1} \text{ s}^{-1}$ ) [44]. On the other hand, although FLX has a lower total removal value than FLXSO<sub>4</sub> in natural water, a much more significant removal difference is observed when the aqueous matrix is altered. This behavior can be explained due to the interaction of the different counterions with the species present in the medium (Table S1). Similarly [45], the evaluated FLX photodegradation of FLX in partially nitrated wastewater during UV irradiation. The authors demonstrated that the presence of nitrite in the wastewater matrix during UV irradiation enhanced FLX degradation. According to these authors, reactive species, such as HO<sup>•</sup> generated in wastewater, are responsible for promoting the photoreactions of the drug. Another important point that is reinforced by this behavior is the hypothesis that there is greater kinetic competition between FLXSO<sub>4</sub> and organic matter, leading to a less expressive increase in removal with the change of the matrix from pure water to natural. Despite this, the high FLXSO<sub>4</sub> removal values in the natural water sample indicate the susceptibility of fluoxetine to be degraded in a medium containing sulfate ions.

### 3.3. Photochemical Persistence of FLX versus FLXSO<sub>4</sub> in the Guarapiranga Reservoir

For a better understanding of the environmental persistence of the fluoxetine variants studied in an urban reservoir, simulations of photochemical persistence were carried out using the conditions of the Guarapiranga reservoir in two specific periods of 2021 (June and September). As can be seen in Figure 4, small variations in half-life times are attributed to seasonal changes (June to September). This can be explained by the fact that the real parameters used in the simulations present a low variation between these months, except for the values of turbidity, total chlorine, and chlorophyll-*a* (Table 1).

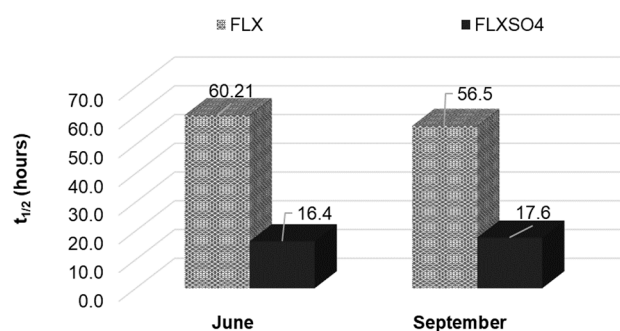


**Figure 4.** Predicted variation of ANT half-life times in the Guarapiranga Reservoir in June and September 2021.

Taking into account the locally measured data from the Interlagos meteorological monitoring station (23°43'12" S, 46°40'48" W), managed by the Instituto Nacional de Meteorologia (INMET), half-life estimates were, on average, five days higher than the values predicted using typical meteorological year (TMY) data. Therefore, atmospheric effects can be satisfactorily simulated using TMY data, and this approach was adopted in the simulations.

A subtle reduction in half-life from June to September ( $t_{1/2 \text{ June}} = 60.2 \text{ h}$ ;  $t_{1/2 \text{ September}} = 56.5 \text{ h}$ ) occurred for FLX (Figure 4). It is possible to associate this result with the occurrence of cloudier days in June (Figure S2), thus reducing insolation and inhibiting direct and indirect photolytic processes. In contrast, although days were generally warmer and sunnier in September (Figure S2), few differences were observed regarding photochemical persistence due to a low contribution of direct photolysis in the removal of FLX in both months (Figure 5). Parameters such as TOC, chlorophyll-*a*, turbidity, and total chlorine concentration were higher in this month (Table 1), possibly increasing eutrophication [30,40],

which also negatively affects direct and indirect photolysis. However, biodegradation had a greater impact on half-lives than eutrophication for FLX, especially in the month of June (Figure 5a). In addition, it is worth noting the high values of TOC and nitrates observed in September (Table 1) that directly influence indirect photolytic processes, which justify a lower persistence of FLX and an increase in FLX removal routes by  $\text{HO}^\bullet$  and  ${}^3\text{CDOM}^*$  in this month (Figure 5b).

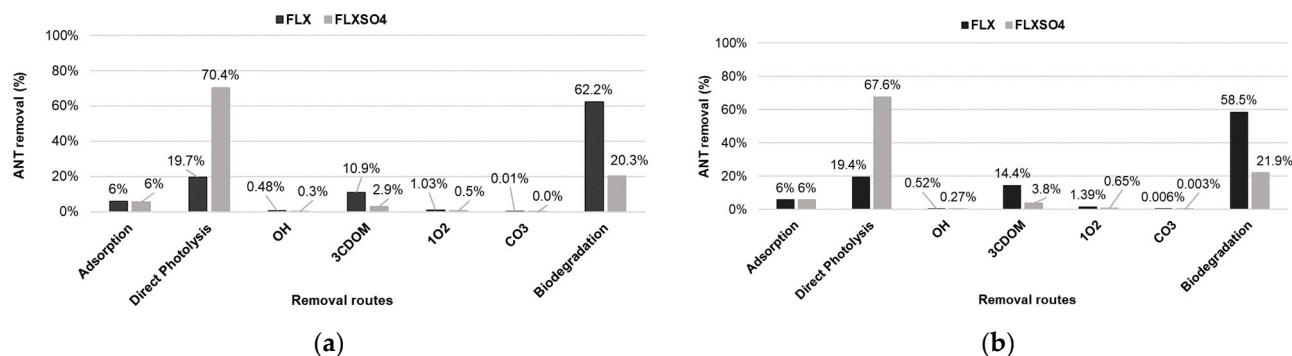


**Figure 5.** Contribution of each degradation pathway in the removal of the pollutants from the reservoir water. (a) June; (b) September.

Shorter half-lives were obtained for FLXSO<sub>4</sub> ( $t_{1/2}$  June = 16.4 h;  $t_{1/2}$  September = 17.6 h) when compared to FLX (Figure 4). This may be associated with the interactions between the reactive species formed and the antidepressant molecules in the presence of different counter-anions ( $\text{Cl}^-$  and  $\text{SO}_4^{2-}$ ). Therefore, as the kinetic constants obtained in competition kinetic experiments for both FLX and FLXSO<sub>4</sub> presentations take into account the presence of the respective counter-anion, the kinetic model predictions of half-lives indirectly also consider such interactions. In addition, it is possible to associate these results with a more pronounced FLXSO<sub>4</sub> direct photolysis route in the two scenarios studied (Figure 5), which is the main contributing factor to the reduction in persistence. Conversely, FLXSO<sub>4</sub> showed a higher persistence in the month of September, being more sensitive to eutrophication processes that directly affect the availability of light (Figure 5b). In turn, the biodegradation route is a less pronounced removal factor for FLXSO<sub>4</sub> compared to FLX. Furthermore, pathways such as the reaction with  ${}^3\text{CDOM}^*$  are even less pronounced for FLXSO<sub>4</sub>, as corroborated by the experimental data (Table 2).

It is important to note that the adsorption phenomenon has a negligible effect on contaminant removal. When not considered, a small change in the half-life values was observed (FLX:  $t_{1/2}$  June = 60.1 h;  $t_{1/2}$  September = 52.5 h; FLXSO<sub>4</sub>:  $t_{1/2}$  June = 16.1 h;  $t_{1/2}$  September = 16.9 h). On the other hand, greater persistence is expected when adsorption and biodegradation are not considered in the simulations (FLX:  $t_{1/2}$  June = 110.1 h;  $t_{1/2}$  September = 113.3 h; FLXSO<sub>4</sub>:  $t_{1/2}$  June = 34.5 h;  $t_{1/2}$  September = 36.5 h), suggesting biodegradation as an important mechanism in the removal of the target contaminants.

#### 4. Conclusions

Direct photolysis experiments in pure water showed that the sulfate-modified form of fluoxetine (FLXSO<sub>4</sub>) is more sensitive to direct photolysis since the counterion modification allows for a higher molar absorption coefficient in the irradiation range. Competition kinetic studies revealed that reactions with  $\text{HO}^\bullet$  and  ${}^3\text{CDOM}^*$  are more important than those with  ${}^1\text{O}_2$  in the degradation of the antidepressants studied (FLX and FLXSO<sub>4</sub>). However, FLXSO<sub>4</sub> showed a lower rate with  ${}^3\text{CDOM}^*$ , leading to the hypothesis that the modification of the counterion provides greater kinetic competition with organic matter. Experiments in a real water matrix showed that other reactive species in the medium can positively contribute to the degradation of the antidepressant, with FLXSO<sub>4</sub> being even more expressive, possibly due to the synergistic effect of the sulfate counterions, suggesting that the presence of these ions in the medium can contribute to the formation of reactive

species that promote fluoxetine removal. Through the half-life analysis, the results of the kinetic simulations revealed that the time of year was not an important influencing factor on persistence since the actual parameters did not show such significant changes between the study months. In addition, a negligible effect on the removal of contaminants was observed by adsorption effects. However, the increase in the environmental persistence of the antidepressant is closely linked to eutrophication and weather conditions. As a result, the half-life of FLXSO<sub>4</sub> decreased in June, driven by direct photolysis and biodegradation. Therefore, the removal of fluoxetine is strongly driven by the interaction with the reactive species formed, especially when sulfate ions are present in the medium.

**Supplementary Materials:** The following supporting information can be downloaded at: <https://www.mdpi.com/article/10.3390/w14213536/s1>, Figure S1. Experimental setup used to study the photodegradation of antidepressants under simulated sunlight. (1) Thermostatic bath; (2) Jacketed beaker; (3) Irradiation source; (4) Distribution arrangement of vials in the beaker; Figure S2. Pluviometric and radiometric data of the studied site for the simulation period (2021). Daily rainfall and radiometric data were collected from the automatic weather station in the vicinity of the Guarapiranga reservoir, maintained by the Instituto Nacional de Meteorologia (INMET). The original data are provided as total global horizontal irradiance per hour. The data were integrated over the hours to evaluate the total daily irradiance; Figure S3. Hydrolysis of FLX in pure water. Conditions: [FLX]<sub>0</sub> = (10.22 ± 0.25) mg L<sup>-1</sup>; natural pH (~6.7); Figure S4. Hydrolysis of FLXSO<sub>4</sub> in pure water. Conditions: [FLXSO<sub>4</sub>]<sub>0</sub> = (10.34 ± 0.30) mg L<sup>-1</sup>; natural pH (~6.3); Table S1. Physicochemical parameters of the Guarapiranga Reservoir water. Point GUAR00100 (23°45'15" S, 46°43'37" W). Samples collected on 05/30/2022. Table S2. Retention times (RT), limits of detection (LOD), and limits of quantification (LOQ) of the compounds used in the study. References [46–48] are cited in the Supplementary Materials.

**Author Contributions:** Conceptualization, L.P.S.; methodology, L.P.S.; software, J.G.M.C. and B.R.; validation, A.M.L.-A. and B.R.; formal analysis, L.P.S.; investigation, L.P.S.; resources A.C.S.C.T.; data curation, L.P.S., A.M.L.-A., B.R. and A.C.S.C.T.; writing—original draft preparation, L.P.S.; writing—review and editing, A.M.L.-A., B.R. and A.C.S.C.T.; visualization, L.P.S.; supervision, A.M.L.-A., B.R. and A.C.S.C.T.; project administration, A.C.S.C.T.; funding acquisition, A.C.S.C.T. All authors have read and agreed to the published version of the manuscript.

**Funding:** This research was funded in part by the Coordenação de Aperfeiçoamento de Pessoal de Nível Superior—Brasil (CAPES)—Finance Code 001. The authors thank the support of the São Paulo Research Foundation (FAPESP) [grant number 2019/24158–9] and the National Council for Scientific and Technological Development—Brazil (CNPq) [grant number 311230/2020–2].

**Institutional Review Board Statement:** Not applicable.

**Informed Consent Statement:** Not applicable.

**Data Availability Statement:** Not applicable.

**Acknowledgments:** The authors thank the support of the (São Paulo) State Environmental Company (CETESB), Paulo de Sousa Carvalho Junior from the Physics Institute of the Federal University of Mato Grosso do Sul (UFMS), and Marcela Prado Silva Parizi from the São Paulo State University (UNESP).

**Conflicts of Interest:** The authors declare no conflict of interest. The funders had no role in the design of the study; in the collection, analyses, or interpretation of data; in the writing of the manuscript; or in the decision to publish the results.

## References

1. Castillo-Zacarias, C.; Barocio, M.E.; Hidalgo-Vázquez, E.; Sosa-Hernández, J.E.; Parra-Arroyo, L.; López-Pacheco, I.Y.; Barceló, D.; Iqbal, H.N.M.; Parra-Saldívar, R. Antidepressant drugs as emerging contaminants: Occurrence in urban and non-urban waters and analytical methods for their detection. *Sci. Total Environ.* **2021**, *757*, 1–16. [[CrossRef](#)] [[PubMed](#)]
2. Melchor-Martínez, E.M.; Jiménez-Rodríguez, M.G.; Martínez-Ruiz, M.; Peña-Benavides, S.A.; Iqbal, H.M.N.; Parra-Saldívar, R.; Sosa-Hernández, J.E. Antidepressants surveillance in wastewater: Overview extraction and detection. *Case Stud. Chem. Environ. Eng.* **2021**, *3*, 100074. [[CrossRef](#)]

3. Fuentes, A.; Pineda, M.; Venkata, K. Comprehension of top 200 prescribed drugs in the US as a resource for pharmacy teaching, training and practice. *Pharmacy* **2018**, *6*, 43. [[CrossRef](#)] [[PubMed](#)]
4. Lajeunesse, A.; Smyth, S.A.; Barclay, K.; Sauv e, S.; Gagnon, C. Distribution of antidepressant residues in wastewater and biosolids following different treatment processes by municipal wastewater treatment plants in Canada. *Water Res.* **2012**, *46*, 5600–5612. [[CrossRef](#)] [[PubMed](#)]
5. Ram rez-Morales, D.; Masis-mora, M.; Montiel, J.R.; Cambronero-heinrichs, J.C.; Brice o, S.; Rojas-S nchez, C.E.; M ndez-Rivera, M.; Arias-Mora, V.; Tormo-Budowski, R.; Brenes, L.; et al. Occurrence of pharmaceuticals, hazard assessment and ecotoxicological evaluation of WWTPs in Costa Rica. *Sci. Total Environ.* **2020**, *746*, 141200. [[CrossRef](#)] [[PubMed](#)]
6. Boogaerts, T.; Degreef, M.; Covaci, A.; Van Nuijs, A.L. Development and validation of an analytical procedure to detect spatio-temporal differences in antidepressant use through a wastewater-based approach. *Talanta* **2019**, *200*, 340–349. [[CrossRef](#)]
7. Ng, K.T.; Rapp-Wright, H.; Egli, M.; Hartmann, A.; Steele, J.C.; Sosa-Hern ndez, J.E.; Parra-Saldivar, R. High-throughput multi-residue quantification of contaminants of emerging concern in wastewaters enabled using direct injection liquid chromatography-tandem mass spectrometry. *J. Hazard. Mater.* **2020**, *398*, 122933. [[CrossRef](#)]
8. Lindim, C.; van Gils, J.; Georgieva, D.; Mekenyan, O.; Cousins, I.T. Evaluation of Human Pharmaceutical Emissions and Concentrations in Swedish River Basins. *Sci. Total Environ.* **2016**, *572*, 508–519. [[CrossRef](#)]
9. Pa ga, P.; Santos, L.H.; Ramos, S.; Jorge, S.; Silva, J.G.; Delerue-Matos, C. Presence of Pharmaceuticals in the Lis River (Portugal): Sources, Fate and Seasonal Variation. *Sci. Total Environ.* **2016**, *573*, 164–177. [[CrossRef](#)]
10. Cortez, F.S.; Souza, L.S.; Guimar es, L.L.; Pusceddu, F.H.; Maranh o, L.A.; Fontes, M.K.; Moreno, B.B.; Nobre, C.R.; Abessa, D.M.S.; Cesar, A.; et al. Marine contamination and cytogenotoxic effects of fluoxetine in the tropical brown mussel *Perna perna*. *Mar. Pollut. Bull.* **2019**, *141*, 366–372. [[CrossRef](#)]
11. Glaser, C.; Zarfl, C.; Werneburg, M.; B ockmann, M.; Zwiener, C.; Schwientek, M. Temporal and spatial variable in-stream attenuation of selected pharmaceuticals. *Sci. Total Environ.* **2020**, *741*, 139514. [[CrossRef](#)] [[PubMed](#)]
12. Telles-Correia, D.; Guerreiro, D.F.; Coentre, R.; Zuzarte, P.; Figueira, L. Psicof rmaco na doen a m dica: Cardiologia, Nefrologia, Hepatologia. *Acta M dica Portuguesa* **2009**, *22*, 797–808. [[PubMed](#)]
13. Fernandes, M.J.; Pa ga, P.; Silva, A.; Llaguno, C.P.; Carvalho, M.; V zquez, F.M.; Delerue-Matos, C. Antibiotics and antidepressants occurrence in surface waters and sediments collected in the north of Portugal. *Chemosphere* **2020**, *239*, 124729. [[CrossRef](#)] [[PubMed](#)]
14. Kumar, R.; Kumar, P. Wastewater Stabilisation Ponds: Removal of emerging contaminants. *J. Sustain. Dev. Energy Water Environ. Syst.* **2020**, *8*, 344–359. [[CrossRef](#)]
15. Mackul’ak, T.; Medveck a, E.; Vojs Sta nov a, A.; Brandeburov a, P.; Grabic, R.; Golovko, O.; Marton, M.; Bod k, I.; Medvedov a, A.; G l, M.; et al. Boron doped diamond electrode—The elimination of psychoactive drugs and resistant bacteria from wastewater. *Vacuum* **2020**, *171*, 108957. [[CrossRef](#)]
16. Giannakis, S.; Hendaoui, I.; Jovic, M.; Grandjean, D.; Alencastro, L.F.; Girault, H.; Pulgarin, C. Solar photo-Fenton and UV/H<sub>2</sub>O<sub>2</sub> processes against the antidepressant venlafaxine in urban wastewaters and human urine. Intermediates formation and biodegradability assessment. *Chem. Eng. J.* **2017**, *308*, 492–504. [[CrossRef](#)]
17. Gornik, T.; Carena, L.; Kosjek, T.; Vione, D. Phototransformation study of the antidepressant paroxetine in surface waters. *Sci. Total Environ.* **2021**, *774*, 145380. [[CrossRef](#)]
18. Lastre-Acosta, A.M.; Barberato, B.; Parizi, M.P.S.; Teixeira, A.C.S.C. Direct and indirect photolysis of the antibiotic enoxacin: Kinetics of oxidation by reactive photo-induced species and simulations. *Environ. Sci. Pollut. Res.* **2019**, *26*, 4337–4347. [[CrossRef](#)]
19. Bodrato, M.; Vione, D. APEX (Aqueous Photochemistry of Environmentally occurring Xenobiotics): A free software tool to predict the kinetics of photochemical processes in surface waters. *Environ. Sci. Process. Impacts* **2014**, *16*, 732–740. [[CrossRef](#)]
20. Vione, D. A Critical view of the application of the APEX software (Aqueous Photochemistry of Environmentally-Occurring Xenobiotics) to predict photoreaction kinetics in surface freshwaters. *Molecules* **2020**, *25*, 9. [[CrossRef](#)]
21. Vione, D.; Das, R.; Rubertelli, F.; Maurino, V.; Minero, C.; Barbati, S.; Chiron, S. Modelling the occurrence and reactivity of hydroxyl radicals in surface waters: Implications for the fate of selected pesticides. *Int. J. Environ. Anal. Chem.* **2010**, *90*, 260–275. [[CrossRef](#)]
22. Bacilieri, F.; Vahatalo, A.V.; Carena, L.; Wang, M.; Gao, P.; Minella, M.; Vione, D. Wavelength trends of photoproduction of reactive transient species by chromophoric dissolved organic matter (CDOM), under steady-state polychromatic irradiation. *Chemosphere* **2022**, *306*, 135502. [[CrossRef](#)] [[PubMed](#)]
23. Foote, C.S.; Valentine, J.S.; Greenberg, A.; Liebman, J.F. *Active Oxygen in Chemistry*, 1st ed.; Blackie Academic and Professional; Springer: Berlin/Heidelberg, Germany, 1995. [[CrossRef](#)]
24. McNeill, K.; Canonica, S. Triplet state dissolved organic matter in aquatic photochemistry: Reaction mechanisms, substrate scope, and photophysical properties. *Environ. Sci. Process. Impacts* **2016**, *18*, 1381–1399. [[CrossRef](#)] [[PubMed](#)]
25. Calza, P.; Jim nez-Holgado, C.; Coha, M.; Chromatopoulos, C.; Dal Bello, F.; Medana, C.; Sakkas, V. Study of the photoinduced transformations of sertraline in aqueous media. *Sci. Total Environ.* **2021**, *756*, 143805. [[CrossRef](#)] [[PubMed](#)]
26. Gornik, T.; Vozic, A.; Heath, E.; Trontelj, J.; Roskar, R.; Zigon, D.; Vione, D.; Kosjek, T. Determination and photodegradation of sertraline residues in aqueous environment. *Environ. Pollut.* **2020**, *256*, 113431. [[CrossRef](#)] [[PubMed](#)]

27. Souza, L.P.; Sanches-Neto, F.O.; Junior, G.M.Y.; Ramos, B.; Lastre-Acosta, A.M.; Carvalho-Silva, V.H.; Teixeira, A.C.S.C. Photochemical environmental persistence of venlafaxine in an urban water reservoir: A combined experimental and computational investigation. *Process Saf. Environ. Prot.* **2022**, *166*, 478–490. [CrossRef]
28. Lam, M.W.; Young, C.J.; Mabury, S.A. Aqueous photochemical reaction kinetics and transformations of fluoxetine. *Environ. Sci. Technol.* **2005**, *39*, 513–522. [CrossRef]
29. Vione, D.; Scozzaro, A. Photochemistry of surface fresh waters in the framework of climate change. *Environ. Sci. Technol.* **2019**, *53*, 7945–7963. [CrossRef]
30. CETESB. InfoÁGUAS Portal. Environmental Company of the State of São Paulo (Portal InfoÁGUAS. Companhia Ambiental do Estado de São Paulo). Available online: <https://sistemainfoaguas.cetesb.sp.gov.br/> (accessed on 30 May 2022).
31. Shemer, H.; Sharpless, C.M.; Elovitz, M.S.; Linden, K.G. Relative rate constants of contaminant candidate list pesticides with hydroxyl radicals. *Environ. Sci. Technol.* **2006**, *40*, 4460–4466. [CrossRef]
32. Mostafa, S.; Rosario-Ortiz, F.L. Singlet oxygen formation from wastewater organic matter. *Environ. Sci. Technol.* **2013**, *47*, 8179–8186. [CrossRef]
33. Elovitz, M.S.; Gunten, V.U. Hydroxyl radical ozone ratios during ozonation processes. I. the Rct concept. *Ozone Sci. Eng.* **1999**, *21*, 239–260. [CrossRef]
34. Al Housari, F.; Vione, D.; Chiron, S.; Barbati, S. Reactive photoinduced species in estuarine waters. Characterization of hydroxyl radical, singlet oxygen and dissolved organic matter triplet state in natural oxidation processes. *Photochem. Photobiol. Sci.* **2010**, *9*, 78–86. [CrossRef]
35. Lastre-Acosta, A.M.; Cristofoli, B.S.; Parizi, M.P.S.; Nascimento, C.A.O.; Teixeira, A.C.S.C. Photochemical persistence of sulfa drugs in aqueous medium: Kinetic study and mathematical simulations. *Environ. Sci. Pollut. Res.* **2021**, *28*, 23887–23895. [CrossRef]
36. Gueymard, C.A. SMARTS2: A Simple Model of the Atmospheric Radiative Transfer of Sunshine: Algorithms and Performance Assessment; Rep No. FSEC-PF-270-95; Florida Solar Energy Center: Cocoa, FL, USA, 1995; pp. 1–84.
37. Šúri, M.; Huld, T.A.; Dunlop, E.D. PV-GIS: A web-based solar radiation database for the calculation of PV potential in Europe. *Int. J. Sustain. Energy* **2005**, *24*, 55–67. [CrossRef]
38. Brown, R. Relationships between suspended solids, turbidity, light attenuation, and algal productivity. *Lake Reserv. Manag.* **1984**, *1*, 198–205. [CrossRef]
39. Pompêo, M.; Padial, P.R.; Mariani, C.F.; Cardoso-Silva, S.; Moschini-Carlos, V.; Silva, D.C.V.R.D.; de Paiva, T.C.B.; Brandimarte, A.L. Biodisponibilidade de metais no sedimento de um reservatório tropical urbano (reservatório Guarapiranga—São Paulo (SP), Brasil): Há toxicidade potencial e heterogeneidade espacial? *Geochim. Bras.* **2013**, *27*, 104. Available online: <https://www.geobrasiliensis.org.br/geobrasiliensis/article/view/364> (accessed on 30 August 2022). [CrossRef]
40. CETESB. Environmental Company of the State of São Paulo (Atlas de Cianobactérias da Bacia do Alto Tietê). Available online: <https://www.cetesb.sp.gov.br> (accessed on 8 March 2022).
41. Strain, H.H.; Thomas, M.R.; Katz, J.J. Spectral absorption properties of ordinary and fully deuteriated chlorophylls-a and b. *Biochim. Biophys. Acta* **1963**, *75*, 306–311. [CrossRef]
42. Schwarzenbach, R.P.; Gschwend, P.M.; Imboden, D.M. *Environmental Organic Chemistry*, 2nd ed.; John Wiley & Sons, Inc.: New Hoboken, NJ, USA, 2003.
43. Carena, L.; Puscasu, C.G.; Comis, S.; Sarakha, M.; Vione, D. Environmental photodegradation of emerging contaminants: A re-examination of the importance of triplet-sensitised processes, based on the use of 4-carboxybenzophenone as proxy for the chromophoric dissolved organic matter. *Chemosphere* **2019**, *237*, 124476. [CrossRef]
44. Nunes, R.F.; Metolina, P.; Teixeira, A.C.S.C. Dodecylpyridinium chloride removal by persulfate activation using UVA radiation or temperature: Experimental design and kinetic modeling. *Environ. Sci. Pollut. Res.* **2021**, *28*, 68229–68243. [CrossRef]
45. Hora, P.I.; Novak, P.J.; William, A.A. Photodegradation of pharmaceutical compounds in partially nitrated wastewater during UV irradiation. *Environ. Sci. Water Res. Technol.* **2019**, *5*, 897–909. [CrossRef]
46. Liu, W.C.; Hsu, M.H.; Chen, S.Y.; Wu, C.R.; Kuo, A.Y. Water column light attenuation in Danshuei river estuary, Taiwan. *J. Am. Water Resour. Assoc.* **2005**, *41*, 425–436. [CrossRef]
47. Magazinovic, R.S.; Nicholson, B.C.; Mulcahy, D.E.; Davey, D.E. Bromide levels in natural waters: Its relationship to levels of both chloride and total dissolved solids and the implications for water treatment. *Chemosphere* **2004**, *57*, 329–335. [CrossRef]
48. Mansouri, K.; Grulke, C.M.; Judson, R.S.; Williams, A.J. OPERA models for predicting physicochemical properties and environmental fate endpoints. *J. Cheminformatics* **2018**, *10*, 10. [CrossRef]